Accepted Manuscript

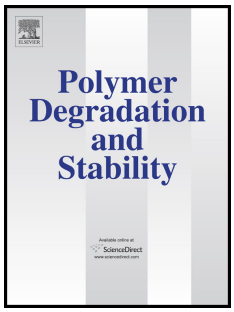

Title: UV degradation of deoxyribonucleic acid

Authors: Paulo J. Gomes, Paulo A. Ribeiro, David Shaw, Nigel J. Mason, Maria Raposo

PII: S0141-3910(09)00324-3

DOI: 10.1016/j.polymdegradstab.2009.09.013

Reference: PDST 5833

To appear in: *Polymer Degradation and Stability*

Received Date: 9 July 2009

Revised Date: 4 September 2009

Accepted Date: 24 September 2009

Please cite this article as: Gomes PJ, Ribeiro PA, Shaw D, Mason NJ, Raposo M. UV degradation of deoxyribonucleic acid, Polymer Degradation and Stability (2009), doi: 10.1016/j.polymdegradstab.2009.09.013

PDST-D-09-00412R1 Ready

UV degradation of deoxyribonucleic acid

Paulo J. Gomes[1], Paulo A. Ribeiro[1], David Shaw[2], Nigel J. Mason[3] and Maria Raposo[1*]

[1]CEFITEC, Departamento de Física, Faculdade de Ciências e Tecnologia, Universidade Nova de Lisboa, 2829-516 Caparica, Portugal

[2]Daresbury Laboratory, Daresbury Science & Innovation Campus, Warrington, Cheshire, WA4 4AD, UK

[3]Department of Physics and Astronomy, The Open University, Walton Hall, Milton Keynes MK7 6AA, UK

*Departamento de Física, Faculdade de Ciências e Tecnologia, Universidade Nova de Lisboa, Campus de Caparica, 2829-516 Caparica Fax: +351212948549; E-mail: mfr@fct.unl.pt

ABSTRACT The effects of UV synchrotron radiation on deoxyribonucleic acid (DNA) cast films have been systematically investigated by vacuum ultraviolet and infrared spectrophotometry as a function of irradiation time. Cast DNA films exposed at 140 nm (8.85 eV) for different irradiations times, revealed consistent changes in their VUV spectra which indicate a decrease of thymine groups and an increase of $\pi \rightarrow \pi^*$ transition spectral signature associated with the C=O group of the open sugar chain. This result was corroborated by a decrease in C-O stretching vibration at 1061 cm^{-1} observed in the infrared spectra. Both these results are consistent with the creation of single strand breaks in the deoxyribose component of DNA molecule and a decrease in the phosphate groups. It was also shown that UV radiation is effective in damaging the thymine groups involved in Hoogsteen base pairing with adenine. The analysis of the infrared data suggests that the usual spectroscopic fingerprints of DNA denaturation are not necessarily a reliable measure of DNA damage.

Keywords: DNA, Cast film, Ultraviolet radiation, Radiation damage, Deoxydeoxyribose, Hoogsteen base pairing.

INTRODUCTION

Radiation induced damage in biomolecules is currently a hot topic in molecular physics since research has shown that irradiation with particle/photon energies below the ionizing potential can induce damage in deoxyribonucleic acid (DNA)[1]. However, how such radiation damage is induced at molecular level still not well understood [2]. When ionizing radiation interacts with matter it produces, in very short times (femtoseconds), a large number of ions, radicals, excited neutrals and ballistic secondary electrons with initial kinetic energies below 100 eV [3,4], which can subsequently cause both physical and chemical modification in the biological media. Furthermore it has recently been shown that secondary electrons with energies between 4 to 6 eV can induce strand break formation in double-stranded supercoiled DNA [5]. Major experimental and theoretical studies have sought to determine the interaction mechanisms leading to such low energy and damage at the molecular level and dissociative electron attachment is now believed to be dominant mechanism. Complementary studies on effect radiation damage in DNA plasmid have been performed using 7-150 eV synchrotron radiation [6] and results have revealed that DNA single-strand (SSB) and double-strand (DSB) breaks occur at all these measured energies, for both dry and solution plasmid DNA, with tissue damage being induced in the presence of water molecules which is more representative of the situation in real cells [7], as OH radicals are released to undertake chemical rather than direct physical attack on the DNA. It should be remarked here that a large number of studies about free radical chemistry of DNA have been performed [8,9 and references therein], and these studies are fundamental to understand the reaction processes which occur when the DNA molecule is irradiated in presence or not of water molecules.

A new approach is needed in which biological samples are studied in an environment that mimics the cell. This new approach involves the production of functional biomimetic membranes at planar interfaces. It is necessary to keep the membrane in, as far as possible, a natural aqueous environment and, for the sake

of quantitative characterization, it is desirable to have it at a planar solid interface. A methodology to accomplish this is to assemble, from a liquid/solid interface, biological molecules such as lipids, DNA, proteins and enzymes onto solid substrates covered with a soft cushion of adsorbed polyelectrolytes having a high water content [10,11]. A simple and versatile method for producing these architectures is the sequential build up of layers of functional materials by the layer-by-layer (LBL) technique [12,13]. This technique, initially applied to the production of polyelectrolyte thin films, has also been found to be suitable for the production of functionalized biomolecular architectures [14,15,16,17,18] and is therefore a relevant methodology for producing biological mimics to address radiation damage studies. However, it is fundamental to characterize the radiation degradation of the biological macromolecules in vacuum. In this paper, the effect of UV radiation [140 nm] on condensed phase DNA cast films in vacuum is reported. Analysis by both UV and IR spectroscopies allows obtain information about the effect of radiation damage on DNA's constituent molecules. The results indicate that the main damage induced is the rupture of deoxyribose C-O-C bonds leading to the creation of C=O bonds and fragmentation of phosphate groups with damage to the thymine molecules which are involved in Hoogsteen base pairing.

It should be noted that the conditions of DNA as a dry film are far from those of DNA in a living cell, the radiation damage in vacuum conditions being less effective than in wet real conditions where the presence of water molecules is significant and the interaction of water photolysis/radiolysis products with the DNA molecules takes place. However, the characterization of the UV radiation effect (140 nm) on DNA molecules in vacuum as performed in this work is of importance for comparison of the effect of UV radiation on DNA molecules surrounded by water molecules to infer its real contribution for the DNA damage. Actually (data not reported in this article) the amount of water molecules surrounding the DNA molecules is being controlled [19] taking into account the achievements of Lourenço et al [10,11] obtained with

LbL films of common polyelectrolytes prepared from different salted aqueous solutions, and producing DNA LbL films.

Experimental

Cast films were prepared from deoxyribonucleic acid sodium salt from calf thymus (DNA), obtained from Aldrich. DNA was dissolved in ultra-pure water to a concentration of 0.5 mg/mL. The solution was deposited onto calcium fluoride (CaF_2) substrates and dried for 2 hours in vacuum desiccators. The cast DNA films were irradiated for different periods and characterized, after each exposure, using synchrotron radiation at station 3.1 at the Daresbury Synchrotron Facility, UK. The mean light intensity impinging the sample at 140 nm was of the order of $8.5x10^{-4}$ W/m^2. Infrared spectra of the samples were measured using a Fourier transform infrared spectrophotometer Nicolet - model 530.

Results and Discussion

1. Effect of VUV radiation on DNA electronic transitions

The absorbance spectrum of a DNA cast film prepared from aqueous solution deposited onto a CaF_2 substrate is shown in figure 1. Although some evidence for fine structure could seen in the spectrum, two main bands, one at about 260 nm and the other at about 190-200 nm can be observed. The 260 nm band is the well known DNA absorption band generally attributed to the DNA bases [20]. The band centred at about 190-200 nm may be attributed to the adenine peaks at 207 nm (5.90eV) and at 179 nm (6.80 eV) and to thymine base peaks at 208 nm (5.86 eV) and 173.5 nm (7.04 eV) [20]. In order to obtain more information about the peak structure, the spectrum was deconvoluted into a set of Gaussians with the features listed in Table 1. The values displayed in this table correspond to the average of peak positions and widths at half heights calculated using four different spectra. The peak centred at 119.8 nm (10.4 eV) is due to direct ionization of nucleobases

[21]. The peak at 161.8 nm (7.66 eV) arises from strong thymine absorption as determined by Shlukla and Leszczynsky [22]. The peaks at 177.4 nm (6.99 eV), 188.3 nm (6.59 eV) and 201.5 nm (6.15 eV) are due to the strong transitions located at 6.28 (4^1 A'), 6.38 (6^1 A') and 6.81 (8^1 A') calculated by Borin et al [23] for purine N(7)H and N(9)H. The peak 209.9nm (5.91 eV) may be due to n → π* guanine transition and a π → π* transition in thymine [22] and the peak at 263.4 (4.708 eV) is generally assigned to all bases, see for example the recent work of So and Alavi [24], with assignments of vertical excitation energies displayed in [25]. In addition, the DNA molecule spectra should have contributions of deoxyribose and phosphate groups as will be discussed later.

The absorbance spectra obtained before and after different irradiation time periods of DNA cast films with synchrotron radiation are shown in figure 2. The films were irradiated at 140 nm which is close to the first ionization potential of several DNA constituents of about 9 eV [26]. It should be noted that the apparent increase of absorbance with irradiation time is due to an increase in the baseline absorption. Such changes in the baseline upon irradiation might be indicative of fragmentation. Baseline corrected DNA VUV spectra, in the 170 to 230 nm wavelength region, plotted for irradiation times are shown in Figure 3. From these curves one can observe a slight increase in absorbance intensities and change in the behaviour of the absorbance curves after irradiation of the DNA samples which is indicating that some transitions are being promoted.

The DNA spectra for different irradiation times were deconvoluted into Gaussians with the same characteristics as the unirradiated samples (listed in Table 1). The peak areas of each Gaussian were plotted versus the irradiation time as shown in figure 4 a), b) and c). These peak areas were found to decrease with irradiation time for the 162 nm and 263 nm peaks, indicating a decrease of thymine groups. However, one cannot assume that other DNA bases groups are not being affected. An increase of 188 nm and 202 nm peaks areas was also observed which indicates a modification in the DNA molecule. Recently, Nielsen et al. [27] using VUV circular

dichroism measurements on aqueous sugar solutions suggested the presence of a weak band at 188 nm associated with the $\pi \rightarrow \pi^*$ transition of the C=O chromophore in the sugar open-chain. Therefore the increase of absorbance observed at 188 nm can be ascribed to an increase in the C=O groups as a result of formation of sugar open-chains.

Finally, it should be remarked here that after one hour of radiation exposure no further changes are observed in the spectra, which means that under the present experimental conditions irradiation of DNA films with 140 nm light of flux of 8.5×10^{-4} W/m^2 is sufficient to induce DNA damage in 10-15 minutes.

2. Effect of VUV radiation on the vibrational spectra

2.1. DNA band assignments

As the duration of the scan of a VUV spectrum took about 15 to 20 minutes, the measurement of VUV spectra can clearly induce changes in the DNA. For this reason, the effect of the UV radiation on DNA films was further investigated by FTIR spectroscopy. The spectra in the 1800-900 cm^{-1} range of a DNA film before and after 80 minutes of irradiation at 140 nm are shown in figure 5. Three main regions can be observed in these spectra namely, at 1800-1500 cm^{-1}, 1500-1250 cm^{-1} and 1250-900 cm^{-1}. These regions are composed by a set of absorbance peaks components that can be associated with DNA molecular vibrations according the literature [28,29,30], as follows: *a) DNA bases (1800-1500 cm^{-1})* - This range is associated with the DNA bases and contains 6 peaks centred at 1711, 1693, 1651, 1605, 1581 and 1531 cm^{-1}; *b) Base-sugar (1500-1250 cm^{-1})* - This region corresponds to the IR absorption in the bases vibrations and base vibrations influenced by the sugar component. In this region, 8 peaks were found at 1485, 1446, 1414, 1390, 1366, 1297, 1280 and 1241 cm^{-1} ; and *c) Backbone (1250-900 cm^{-1})* - This region is associated with the phosphate backbone region and contains

seven peaks centred at 1210, 1183, 1097, 1061, 1020, 961 and 927 cm^{-1}. The assignments of all these peaks are displayed in Table 2.

Several changes in the IR spectra have seen observed after irradiation. In order to better analyze the infrared spectra changes, spectra baselines were removed and the peaks which did not change as a result of exposure to UV radiation were identified. From this analysis, the peak area at 961 cm^{-1} wavenumber, which is associated with C-C stretch of DNA backbone, was found not to change under UV radiation, so that this peak was used to normalize the obtained data, dividing the other peaks areas by the area of this peak, avoiding the possibility that the small changes due to the measurement of the infrared spectra in different regions of the sample are affecting the observed peak areas decrease or increase.

In order to quantify the changes induced by UV radiation the spectra were fitted with Gaussian components after baseline removal. The peak characteristics namely, peak position and peak width, were calculated as free fitting parameters for each spectrum. Mean values for the peak positions and widths were then calculated from all fitted values and are displayed in Table 2. These mean values were then used in new fittings and the peak areas calculated. The calculated peak areas are essentially proportional to the number of oscillators which lead a particular absorbance peak. These calculations allow us to determine peak area ratios relative to the 961 cm^{-1} peak area, which is associated with the backbone frequency region, as a function of irradiation time. In Table 2 is also displayed the general behaviour with the irradiation time, designed by increase, decrease or constant, of each peak area relative to that under the 961 cm^{-1} peak.

2.2. Damage in DNA sugar related components

Since the VUV spectra results suggested that the UV radiation opens the deoxyribose ring, the related sugar components were investigated. In figure 6, the calculated area ratios of the furanose vibration (1020 cm^{-1}), of the C-O stretching

vibration of nucleic acid sugar (1061 cm^{-1}) and of the PO_2^- stretching of backbone (1097 cm^{-1}) relative to bonds associated with the DNA backbone (961 cm^{-1}) are plotted as a function of irradiation time. This figure reveals that vibrations associated with the furanose are independent of the irradiation time, while those associated with C-O stretching of nucleic acid sugar (1061 cm^{-1}) and PO_2^- stretching vibrations are seen to decrease with the irradiation time. Such a decrease in the C-O bond stretching vibration of deoxyribose during irradiation has also been observed by Tang and Guo [31] in characterizing the effect of UVA and UVB irradiation on aqueous solutions of DNA calf thymus using Raman spectroscopy analysis. Therefore it can be concluded that 140 nm radiation is sufficient to open the sugar ring and to break the DNA phosphate groups. Although both C-O and PO_2^- stretching vibrations decrease with irradiation time the ratio of the peak areas of 1097 cm^{-1} and 1061 cm^{-1} peaks is also seen to decrease with the irradiation time which indicates that the effect of radiation is more dramatic in the PO_2^- groups.

Taking into account these results the ratios of the vibrations associated with the deoxyribose group were plotted as a function of irradiation time, figure 7. The graph shows the normalized peak area ratios for C-O stretching vibration of nucleic acid sugar (1061 cm^{-1}), PO_2^- stretching of backbone (1097 cm^{-1}), antisymmetric PO_2^- stretch in A DNA form (1241 cm^{-1}) and CN3H bend of deoxyribose thymine (1280 cm^{-1}) relative to the CC stretch in the DNA skeleton (961 cm^{-1}). All of these ratios decrease with irradiation time but the radiation effect on the sugar chain is weaker than CN3H bend of deoxyribose thymine (1280 cm^{-1}). The ratio for C-O stretching vibration of nucleic acid sugar (1061 cm^{-1}) decreases by 10%, while the intensity of the CN3H bending mode of deoxyribose thymine (1281 cm^{-1}) decreases by some 40%. This result shows that the effect of UV radiation is located essentially in the deoxyribose thymine groups. In addition, both PO_2^- stretching of backbone (1097 cm^{-1}) and antisymmetric PO_2^- stretch in A-form DNA (1241 cm^{-1}) decrease similarly, confirming the consistency of this method of analysis.

The normalized peak area ratio of the CH3 symmetric stretch with deformation of deoxyribose thymine (1390 cm^{-1}) relative to vibrations associated with DNA skeleton (961 cm^{-1}) also decreases with irradiation time, as is shown in figure 8, where this peak area ratio is plotted together with the normalized ratio of the CN3H bend of deoxyribose thymine (1280 cm^{-1}) peak area relatively to the peak area associated to DNA skeletal vibrations (961 cm^{-1}). Although, the ratio at 1390 cm^{-1} seems to decrease to smaller values, it can be observed that both ratios decrease in a similar way, within the error bars. As both these vibrations are related with deoxyribose thymine vibrations these similar decrease are consistent. For comparison with the effect of UV radiation in cytidines and guanosines, the normalized peak area ratio of the vibrations associated with cytidine and guanosine in anti-conformation (1366 cm^{-1}) and the vibrations associated to DNA skeletal (961 cm^{-1}) is also observed to decrease with irradiation time, as is shown in figure 9, where this peak area ratio is plotted together with the normalized peak area ratio of the CH3 symmetric deformation of deoxyribose thymine (1390 cm^{-1}), relative to the vibrations associated to DNA skeleton. From this plot one can conclude that the UV radiation effect is more severe in the deoxyribose thymines than in the cytidines and guanines.

Related with the deoxyribose a similar decrease in the area ratios of 1414 cm^{-1} and 1446 cm^{-1} peaks, respectively, associated with C3'-endo deoxyribose in A and Z forms helices, and with adenine in A, B and Z forms, can be observed in figure 10. In this figure was also plotted the peak area ratio of the 1280cm^{-1} which is associated C5=C6 vibration of cytidine and to CN3H bend of deoxyribose thymine for comparison. From this comparison, one can see that the decrease in the 1280 cm^{-1} feature is slightly more accentuated indicating that deoxyribose associated to thymines are more affected by the radiation. It should remarked here that DNA molecules are more easily attacked by ozone than are RNA molecules [32,33], suggesting that thymine groups are the DNA components more easily undrgoing damage, which corroborates these conclusions.

2.3. Damage in thymine groups

The above described results suggest that the infrared region associated with the thymine groups should be further explored. Moreover, it is known that two adjacent thymine groups when submitted to UV A and B radiation tend to dimerise. In fact, the cyclobutane pyrimidine dimer is the most abundant lesion caused by ultraviolet radiation and consists of a reaction of the carbon-carbon double bonds of two proximal pyrimidine bases to form a cyclobutane ring. This reaction has been recently investigated by femtosecond time–resolved infrared spectroscopy [34] and it was revealed that in DNA samples irradiated at 266 nm, the intensity of infrared bands due to double-band stretch associated with the two carbonyl groups and the C5=C6, double bond (1632 and 1664 and 1693 cm^{-1}) decreases after several minutes of irradiation. On the other hand, the intensity of some peaks in the range of 1300 to 1500 cm^{-1} is seen to increase with the UV exposure. In the present work, related with the thymine there are three peaks respectively associated with CN3H bend of deoxyribose thymine (1280 cm^{-1}), CH_3 symmetric vibration of deoxyribose thymine (1390 cm^{-1}) and a peak at 1701 cm^{-1}, not listed in table 2, which is the superposition of two peaks, one associated with C2=O2 stretching of thymine in single or double-stranded (1693 cm^{-1}) and other associated to C2=O2 stretching of thymines involved in reverse Hoogsteen third strand binding and/or to C6=O6 stretching of guanines involved in Hoogsteen third strand binding (1711 cm^{-1}). The area of the 1701 cm^{-1} peak was calculated for comparison of the decay of the C2=O2 bond in all thymines. Figure 11 shows the plot of the normalized areas ratios of the peaks at 1280 cm^{-1}, 1390 cm^{-1} and 1711 cm^{-1} relative to the area of the 961 cm^{-1} peak. The peaks associated with both CN3H bend of deoxyribose thymine and CH3 symmetric deformation of deoxyribose thymine decrease by 40% and both showing a similar behaviour with irradiation time, whilst peaks due to C=O stretching of thymine decrease only by 10%.

Changes observed in the thymine group may be seen in the 1675 to 1750 cm^{-1} region, where two Gaussian components were found, taking into account that the C2=O2 strength of thymine single stranded or double stranded is associated to 1693 cm^{-1} vibrations and the C2=O2 stretching of thymines involved in reverse Hoogsteen third strand binding is present as a vibration peak at 1711 cm^{-1}. In figure 12, the normalized 1693 cm^{-1} and 1711 cm^{-1} peak ratios relative to 961 cm^{-1} are plotted. The area ratio considering only a peak at 1701cm^{-1} in this region was also plotted for comparison. From the plot, it can be seen that the UV radiation does not affect the peak at 1693 cm^{-1} associated with C2=O2 strength of thymine, while the C2=O2 stretching of thymines involved in reverse Hoogsteen third strand binding and/or to C6=O6 stretching of guanines involved in Hoogsteen third strand binding [1711 cm^{-1}] is affected. Moreover the decrease of the C=O peak is followed by an increase in the intensity of the 1210 cm^{-1} peak at the same rate of decrease in the 1711 cm^{-1} peak, which can be seen in figure 13. However, here it should be remembered that the peak at 1210 cm^{-1} can be assigned to both antisymmetric PO_2^- stretch in B DNA form and to a normal C-O bond. Since an increase in the B-DNA form is not expected to occur, one can infer that the C=O bone of thymine is being replaced by C-O, which can be accounted by the different spatial distribution of the adenine and thymine and the pairing between them. From the theoretical point of view Cubero et al [35] calculate average hydrogen-bond energies of -13.3 and -12.1 kcal/mol for Hoogsteen and Watson-Crick pairings, respectively, values which are in accordance with the ones calculated by Monajjemi and Chahkandi [36]. In addition, these authors also calculated the dipole moment for both Watson-Crick and Hoogsteen adenine thymine hydrogen bonds and achieved values of about 2 and 8 Debyes, respectively. Similar values for hydrogen bonds can be also found in [37]. Moreover, Kryachko and Sabin [38] investigated the variety of facets of the hydrogen-bond pattern of the Watson-Crick adenine. thymine (A.T) base pair of DNA obtaining the transition state of adenine.thymine which governs the conversion of the Watson.Crick pair of adenine.thymine into the Hoogsteen one and

discussed the energetical and geometrical features of this conversion. In fact, these authors reported the transition state of adenine.thymine between the Watson-Crick and Hoogsteen base pairs of adenine.thymine, where the pairs are disposed nearly perpendicular to each other, being the barrier height, taken relatively to the WC pair comprise a value of 6.5 kcal/mol at the Hartree-Fock computational level and 5.4 kcal/mol at the B3LYP one. Taking into account the described literature, our results show that the presence of Hoogsteen pairings, highly polarisable, contributes for the degradation by UV and the Hoogsteen pairings are not being converted in Watson-Crick pairing as should be suggested by the theory.

2.4. DNA denaturation

Finally, in order to confirm that irradiation leads to DNA denaturation, the ratios of the intensities at 1690 cm^{-1} and 1652 cm^{-1} were evaluated. This ratio has been shown to be representative of denaturation (Miyamoto et al [39]). In fact, these authors in investigating the DNA hybridization and denaturation in aqueous solutions using infrared spectroscopy concluded that the ratio of absorbance of the C=O stretching peak at 1690 cm^{-1} to the absorbance peak at 1660 cm^{-1} provides a metric for DNA hybridization and denaturation. In DNA cast films the band at 1693 cm^{-1} can be assigned to the C6=O6 stretch of base paired guanines plus C2=O2 bond stretching vibration of thymines, while the 1651 cm^{-1} band is assigned to C2=O2 of cytosines plus C4=O4 stretching vibrations of thymines [40 and references therein]. However, when the intensity ratios at these wavenumbers are plotted as shown in figure 14, as a function of the irradiation time only a slight denaturation can be inferred, which is in contrast with the data discussed above. However, changes in DNA molecular conformation have been observed. It have be seen that vibrations associated with the antisymmetric PO_2^- stretch in A form decrease, while there is an increase in the antisymmetric PO_2^- stretch in B DNA form (1210 cm^{-1}). As discussed before this increase can be related to an increase in the C-O bond. These results allow conclude that the ratio proposed by Miyamoto el

al is not necessarily a reliable indication of DNA damage or rather the method is only sensitive to one type of DNA damage. This conclusion is also corroborated by the work of Cataldo [32] which demonstrated that DNA is also remarkably damaged by ozone as revealed by the FTIR spectra of DNA samples submitted to ozone stream which change significantly in whole 700 to 1800 cm^{-1} wavenumber region in comparison with spectra of samples without ozone treatment.

CONCLUSIONS

Vacuum ultraviolet and infrared spectroscopies showed that vacuum synchrotron radiation at 140 nm (8.85 eV) induces damage in calf thymus DNA molecules. Although, only small changes in the VUV spectra were revealed during UV irradiation, spectral deconvolution, allowed us to conclude that the contribution of transitions, associated with the open sugar chain, tend to increase in magnitude during irradiation. At the same time, a decrease in the peaks associated with the DNA bases has been observed. Although such effects could be inferred from measured VUV spectra, this technique is not sensitive enough to characterize DNA damage at a molecular level. Infrared spectra of the samples allowed us to assign observed infrared absorbance peaks to particular DNA molecular vibrations. Analysis of changes in the infrared spectra after irradiation generally, revealed that UV radiation leads to a decrease in the magnitude of the absorbance peaks. A decrease is observed in the C-O stretch of the furanose in backbone, in the PO_2^- groups, in the thymine, cytosine and adenine groups. These changes occur at different rates indicating that several damage processes are involved. UV radiation was shown to affect the thymines involved in reverse Hoogsteen third strand binding which is consistent with the observed decrease C2=O2 stretching of thymines involved in reverse Hoogsteen third strand binding, while the C2=O2 stretching vibration of thymine in single or double-stranded remain unchanged. An increase in the anti-symmetric PO_2^- stretch in B form was also observed which has been related to an increase in the number of C-O bonds. It has been shown that

the spectroscopic fingerprints suggested by Miyamoto et al [39] as characteristic of DNA denaturation are not necessarily a reliable measure of DNA damage and other spectroscopic signatures may be/should be used. Comparison of the obtained results with what is known about free-radical induced damage [8, 9 and references therein] is being done. This study will be fundamental to understand the reactions occurring when the DNA molecules are irradiated. To advance in this study it is fundamental control the amount of water molecules surrounding the DNA molecules which is being done using the LbL technique to produce water containing DNA films and characterize the effect of radiation on them.

ACKNOWLEDGMENTS

The authors thank "Fundação para a Ciência e Tecnologia" (Portugal) for their financial support. MR, PAR and PJG acknowledge visiting fellowships within the Open University, UK. MR acknowledges the Short Term Scientific Mission COST P9 – STSM 02196. PAR acknowledges the support received from the European Science Foundation (ESF) for the activity entitled 'Electron Induced Processing at the Molecular Level'. We are also grateful to the CCLRC for access to the Daresbury facility in the UK.

REFERENCES

[1] Berdys, J.; Anusiewicz, I.; Skurski, P.; Simons, J. *J. Am. Chem. Soc* **2004** 126 6441-6447.
[2] Benderitter, M.; Vincent-Genod, L.; Pouget, J.P.; Voisin, P. *Radiation Research* **2003**, 159, 471-483.
[3] Cobut, V.; Frongillo, Y.; Patau, J.P.; Goulet, T.; Fraser, M.J. ; Jay-Gerin, J.P., *Rad. Phys. Chem.* **1998**, 51, 229-243.
[4] Huels, M.A.; Boudaiffa, B.; Cloutier, P.; Hunting, D.; Sanche, L., *J. Am. Chem. Soc.* **2003**, 125, 4467-4477.
[5] Boudaiffa, B.; Cloutier, P.; Hunting, D.; Huels, M.A.; Sanche, L. *Science* **2000**, 287, 1658-1660.
[6] Folkard, M.; Prise, K.M.; Brocklehurst, B.; Michael, B.D. *J. Phys. B: At. Mol. Opt. Phys.* **1998**, 32, 2753-2761.
[7] Folkard, M.; Prise, K.M. *Acta Physica Polonica A* **2006**, 109, 265-271.
[8] von Sonntag, C. *The Chemical Basis of Radiation Biology*, Taylor & Francis, **1987**.
[9] von Sonntag, C. *Free- Induced DNA Damage and Its Repair-A Chemical Perpective*, Springer-Verlag Berlin Heidelberg, **2006**
[10] Lourenco, J.M.C.; Ribeiro, P.A.; Botelho-do-Rego, A.M.; Braz-Fernandes, F.M.; Moutinho, A.M.C.; Raposo, M. *Langmuir* **2004**, 20, 8103-8109.
[11] Lourenco, J.M.C.; Ribeiro, P.A.; Botelho-do-Rego, A.M.; Raposo, M. *J. Colloid and Interface Sci*, **2007**, 313, 26-33.
[12] Decher, G. *Science* **1997**, 277, 1232-1237.
[13] Oliveira-Jr., O.N.; Raposo, M.; Dhanabalan, A. In *Handbook of Surfaces and Interfaces of Materials*; Nalwa, H.S., Ed; Academic Press, New York, 2001; Vol.4, p 1-63.
[14] Ichinose, I.; Kuroiwa, K.; Lvov, Y.; Kunitake, T. In *Multilayer Thin Films*, Decher, G.; Schlenoff, J.B.; Lehn, J.M., Eds; Wiley-VCH Verlag: Weinheim, 2003; p. 155-174.
[15] Mendelsohn, J.D.; Yang, S.Y.; Hiller, J.A.; Hochbaum, A.I.; Rubner, M.F. *Biomacromolecules* **2003**, 4, 96-106.
[16] Jessel, N. *Adv. Materials* **2003** 15, 692-95.
[17] N. Benkirane-Jessel, *Adv. Functional Materials*, **2004**, 14, 174-182.
[18] Ariga, K., Nakanishi, T.; Michinobu, T. *J Nanosci. Nanotechnol.* **2006**, 6, 1718-1730.
[19] Raposo, M.; Gomes, P. J.; Lourenco, J. M. C.; Coelho, M.; Hoffmann, S. V.; do Rego, A. M. Botelho; McCullough, R. W.; Mason, N. J.; Lage, C.;Limao-Vieira, P.; Ribeiro, P. A. AIP Conference Proceedings **2008,** 1080, 125-131.
[20] Isaacson, M. *J. Chem. Phys.* **1972**, 56, 1803-1812.
[21] Roca-Sanjuán, D.; Rubio, M.; Merchán, M.; Serrano-Andrés, L. *J. Chem. Phys.* **2006**, 125, 084302.
[22] Shukla, M.K.; Leszczynski, J. *J. Comp. Chem.* **2004**, 25, 768-778.
[23] Borin, A.C.; Serrano-Andrés, L.; Fülscher, M.P.; Roos, B.O. *J. Phys. Chem. A* **1999**, 103, 1838-1845.
[24] So, R.; Alavi, S. *J. Chem.* **2007**, 28, 1776-1782.
[25] Roca-Sanjuán, D.; Rubio, M.; Merchán, M.; Serrano-Andrés, L. *J. Chem. Phys.* **2006**, 125, 084302.
[26] Tasaki, K.; Yang, X.; Urano, S.; Fetzer, S.; LeBreton, P.R. *J. Am. Chem. Soc.* **1990**, 112, 538-548.
[27] Brondsted-Nielsen, S.; Chakraborty, T.; Hoffmann, S.V. *ChemPhysChem* **2005**, 6, 2619-2624.
[28] Gault, N.; Rigaud, O.; Poncy, J.L.; Lefaix, J.L. *Int. J. Radiat. Biol.* **2005**, 81, 767-779
[29] Lindqvist, M.; Sarkar, M.; Winqvist, A.; Rozners, E.; Strömberg, R.; Gräslund, A. *Biochemistry*, **2000**, 39, 1693-1701.

[30] Banyay, M.; Sarkar, M.; Gräslund, A. *Biophys. Chem.* **2003**, 104, 477-488.
[31] Tang,Y.L.; Guo, Z.Y., *Acta Biochim. et Biophys. Sinica* **2005**, 37, 39-46.
[32] Cataldo, F. International Journal of Biological Macromolecules **2006**, 38, 248-254.
[33] Cataldo, F. Polymer Degradation and Stability, **2005**, 89, 274-281.
[34] Schreier, W.J.; Schrader, T.E.; Koller, F.O.; Gilch, P.; Crespo-Hernández, C.E.; Swaminathan, V.N.; Carrel, T.; Zinth, W.; Kohler, B. *Science* **2007**, 315, 625-29
[35] Cubero, E.; Luque, F.J.; Orozco, M. *Biophysical Journal* **2004**, 90, 1000-1008.
[36] Monajjemi, M.; Chahkandi, B. *J Molec Struct: THEOCHEM* **2005**, 714, 43-60.
[37] Sponer, J.; Jurecka, P.; Hobza, P. *J Am Chem Soc* **2004**, 126, 10142-10151.
[38] Kryachko, E.S.; Sabin, J.R. *International Journal of Quantum Chemistry*, **2003**, 91, 695-710.
[39] Miyamoto, K.I.; Ishibashi, K.I.; Yamaguchi, R.T.; Kimura, Y.; Ishii, H.; Niwano, M. *J Appl Phys*, **2006**, 99, 094702.
[40] Sarkar, M.; Dornberger, U.; Rozners, E.; Fritzsche, H.; Strömberg, R.; Gräslund, A. *Biochemistry* **1997**, 36, 15463-71.

TABLE CAPTIONS

Table 1 – Characteristics of peaks observed in DNA cast films by VUV.

Table 2 – Characteristic infrared absorptions in DNA cast films. The Peak Area Ratio Tendency (PART) indicates the increase or decrease with irradiation time of each peak area relatively to the 961 cm^{-1} peak area.

Table 1

Peak Position (nm)	Peak Position (eV)	Peak Width (nm)	Assignment
119.8±1.1	10.4±0.1	42.5±1.4	Direct ionization of nucleobases
161.8±0.8	7.66±0.04	25.5±1.4	Thymine
177.4±0.5	6.99±0.02	12.2±1.0	Purine N(7)H and N(9)H
188.3±0.8	6.59±0.03	17.9±2.1	Purine N(7)H and N(9)H
201.5±1.6	6.15±0.05	11.5±1.6	Purine N(7)H and N(9)H
209.9±0.6	5.91±0.02	21.8±0.6	n→π* guanine π→π* thymine
263.4±0.08	4.708±0.002	42.0±0.2	All bases

Table 2

Wavenumber (cm^{-1})	Peak Width (cm^{-1})	Literature Wavenumber (cm^{-1})	Assignment	PART
Base frequency region				
1711 ± 1	23±1	1715 1712	C6=O6 stretching of guanines involved in Hoogsteen third strand binding and/or C2=O2 stretching of thymines involved in reverse Hoogsteen third strand binding [28]	decrease
1693 ± 1	28±2	1698 - 1691	C2=O2 strength of thymine single stranded or double stranded [28]	constant
1651 ± 1	50.8±0.2	1655 - 1657	C2=O2 strength of cytosine single stranded or double stranded [28]	constant
1605± 1	22.0±0.2	1601	C=N ring vibration of guanine	decrease
1581± 1	33.2±0.5	1590 - 1575 1585	C=N ring vibration of Guanine single stranded or double stranded [28] Ring vibration of guanine and adenine [29]	decrease
1531± 1	19.0± 0.9	1527 - 1520 1530	In-plane vibration of cytosine single stranded or double stranded [28,29]	constant
Base-sugar frequency region				
1485± 1	29.4± 0.5	1495 - 1476	Ring vibration of Adenine and Guanine [28] N7C8H bend of Adenine/Guanine [28]	constant
1446± 1	21.9± 0.5	1457 - 1453 1438 - 1434	Adenine A/B forms [28] Adenine Z form [28]	decrease
1414± 1	27± 2	1413 - 1408	C3'-endo deoxyribose in *A* form helices [28] C3'-endo deoxyribose in *Z* form helices [28]	decrease
1390± 1	23± 2	1389 - 1374	Calc: CH_3 Symmetric deformation of deoxyribose thymine	decrease

			[28]	
1366± 1	21.7± 0.7	1381 - 1369	Cytidine and guanosine in anticonformation [28,29]	decrease
1297± 1	11.9± 0.1	1297 – 1285	C4-NH2 strength of cytosine [28], [29]	decrease
1280± 1	23.3± 0.6	1281 1275	C5=C6 vibration of cytidine [28] CN3H bend of deoxyribose thymine [28]	decrease
1241± 1	37.9± 0.3	1245 - 1235	Antisymmetric PO_2^- stretch in A-form [28]	decrease
Backbone frequency region				
1210± 1	21.2± 0.1	1225 - 1220	Antisymmetric PO_2^- stretch in B-form [28]	increase
1183± 1	20.9± 0.2		A form marker – Sugar phosphate backbone	decrease
1097± 1	36.7± 0.6	1090 - 1085	Symmetric PO_2^- stretching of Backbone [28]	decrease
1061± 1	31.3± 0.7	1069 - 1044	CO stretch of the furanose in backbone [28]	decrease
1020± 1	33.7± 0.4	1020 - 1010	Furanose vibrations [28]	constant
961± 1	20.9± 0.2	970 - 950	CC stretch of the backbone [28]	----
927± 1	25.6± 0.5	930 - 924	Z-form [28]	constant

FIGURE CAPTIONS

Figure 1 – The vacuum ultraviolet absorbance spectrum of a DNA cast sample. The solid lines correspond to spectrum peak structure obtained by fitting of VUV spectrum with a set of Gaussians.

Figure 2 – Absorbance spectra of a DNA cast sample for different irradiation time periods using 140 nm wavelength radiation.

Figure 3 - DNA VUV spectra, after correction for baselines, for different irradiation times in the 170 to 230 nm range.

Figure 4 – Peak area versus the irradiation time for a DNA cast film. Peak centred at: a) 162 nm; b) 188 nm and 202 nm and c) 263 nm.

Figure 5 – Infrared absorbance spectra of a DNA cast sample before and after irradiation with 140 nm UV light for 80 minutes.

Figure 6 – Ratios of the infrared peak areas at 1020 cm^{-1} (furanose vibrations), 1061 cm^{-1} (CO stretch of the furanose in backbone) and 1097 cm^{-1} (symmetric PO_2^- stretching of backbone) relative to the peak area of the 961 cm^{-1} feature. The peak area was calculated from infrared peaks obtained from spectra of DNA cast sample irradiated for different periods of time using 140 nm synchrotron radiation. The solid lines are guidelines.

Figure 7 – Normalized infrared peak area ratios at 1061 cm^{-1}(CO stretch of the furanose in backbone), 1097 cm^{-1} (symmetric PO_2^- stretching of Backbone), 1241 cm^{-1} (antisymmetric PO_2^- stretch in A-form) and 1280 cm^{-1} (C5=C6 vibration of cytidine and CN3H bend of deoxyribose thymine) relative to peak area at 961 cm^{-1}

of a DNA cast sample irradiated for different periods of time with synchrotron radiation at 140 nm. The solid lines are guidelines.

Figure 8 – Normalized infrared peak area ratios at 1280 cm^{-1} (C5=C6 vibration of cytidine and CN3H bend of deoxyribose thymine), 1097 cm^{-1} (symmetric PO_2^- stretching of backbone) and 1241 cm^{-1} (antisymmetric PO_2^- stretch in A form) relative to peak area at 961 cm^{-1} of a DNA cast sample irradiated for different periods of time with synchrotron radiation at 140 nm. The solid lines are guidelines.

Figure 9 - Normalized infrared peak area ratios at 1366 cm^{-1} (cytidine and guanosine in anticonformation) and 1390 cm^{-1} (CH_3 Symmetric deformation of deoxyribose thymine) relative to peak area at 961 cm^{-1} of a DNA cast sample irradiated for different periods of time with synchrotron radiation at 140 nm. The solid lines are guidelines.

Figure 10 - Normalized infrared peak area ratios at 1280 cm^{-1}(C5=C6 vibration of cytidine and CN3H bend of deoxyribose thymine), 1414 cm^{-1} (C3'-endo deoxyribose in *A*-form helices and C3'-endo deoxyribose in *Z* form helices) and 1446 cm^{-1} (adenine A, B and Z forms) relative to peak area at 961 cm^{-1} of a DNA cast sample irradiated for different periods of time with synchrotron radiation at 140 nm. The solid lines are guidelines.

Figure 11 - Normalized infrared peak area ratios at 1280 cm^{-1}(C5=C6 vibration of cytidine and CN3H bend of deoxyribose thymine), 1390 cm^{-1} (CH_3 Symmetric deformation of deoxyribose thymine) and 1701 cm^{-1} (C2=O2 strength of thymine single stranded or double stranded and C6=O6 stretching of guanines involved in Hoogsteen third strand binding and/or C2=O2 stretching of thymines involved in reverse Hoogsteen third strand binding) relative to peak area at 961 cm^{-1} of a DNA

cast sample irradiated for different periods of time with synchrotron radiation at 140 nm. The solid lines are guidelines.

Figure 12 - Normalized infrared peak area ratios at 1693 cm^{-1} (C2=O2 strength of thymine single stranded or double stranded), 1711 cm^{-1} (C6=O6 stretching of guanines involved in Hoogsteen third strand binding and/or C2=O2 stretching of thymines involved in reverse Hoogsteen third strand binding) and 1701 cm^{-1} (C2=O2 strength of thymine single stranded or double stranded and C6=O6 stretching of guanines involved in Hoogsteen third strand binding and/or C2=O2 stretching of thymines involved in reverse Hoogsteen third strand binding) relative to peak area at 961 cm^{-1} of a DNA cast sample irradiated for different periods of time with synchrotron radiation at 140 nm. The solid lines are guidelines.

Figure 13 - Normalized infrared peak area ratios at 1210 cm^{-1} (antisymmetric PO_2^- stretch in B form) and 1711 cm^{-1} (C6=O6 stretching of guanines involved in Hoogsteen third strand binding and/or C2=O2 stretching of thymines involved in reverse Hoogsteen third strand binding) relative to peak area at 961 cm^{-1}, of DNA cast sample irradiated for different periods of time with synchrotron radiation at 140 nm. The solid lines are guidelines.

Figure 14 - Infrared ratio of absorbance intensity at 1690 cm^{-1} relative to absorbance intensity at 1952 cm^{-1} for different periods of time with synchrotron radiation at 140 nm. The solid line corresponds to data fitting with a straight line.

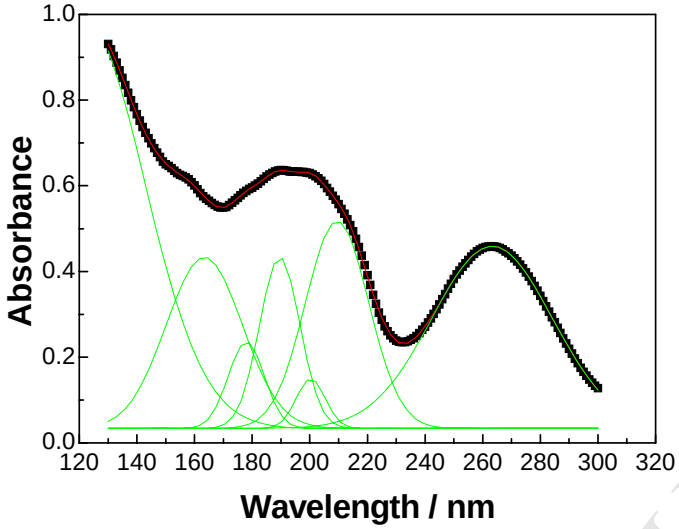

Figure 1 – Paulo J. Gomes et al

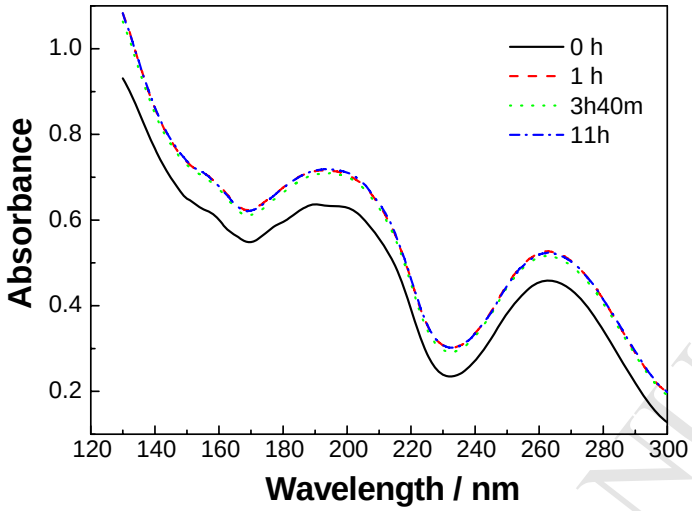

Figure 2 – Paulo J. Gomes et al

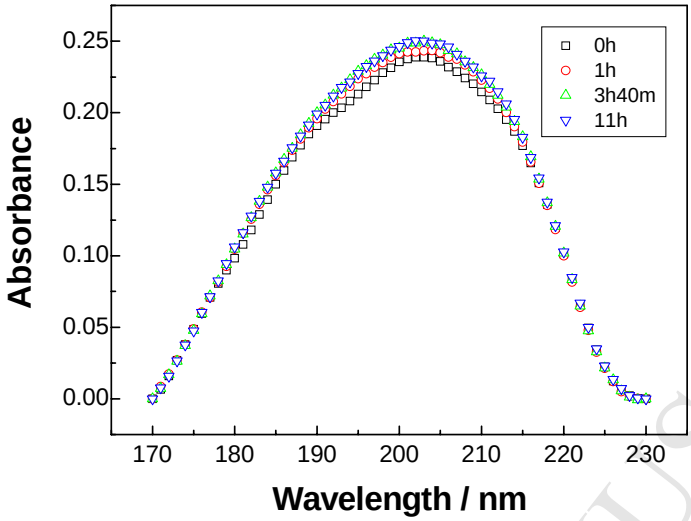

Figure 3 - Paulo J. Gomes et al

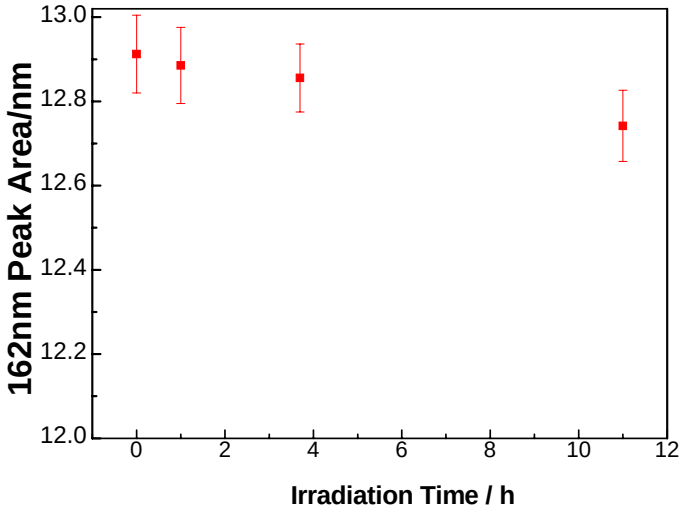

a)

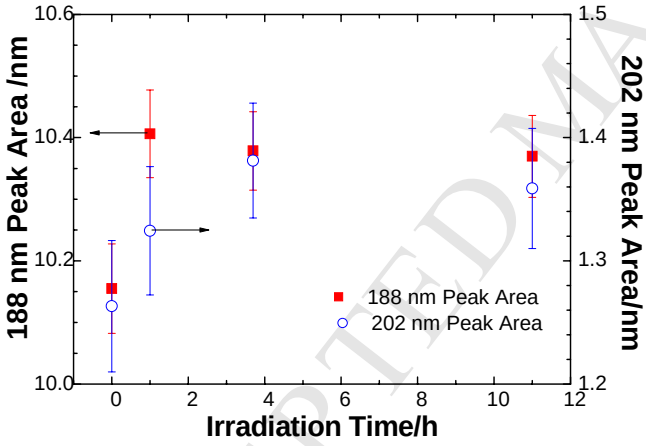

b)

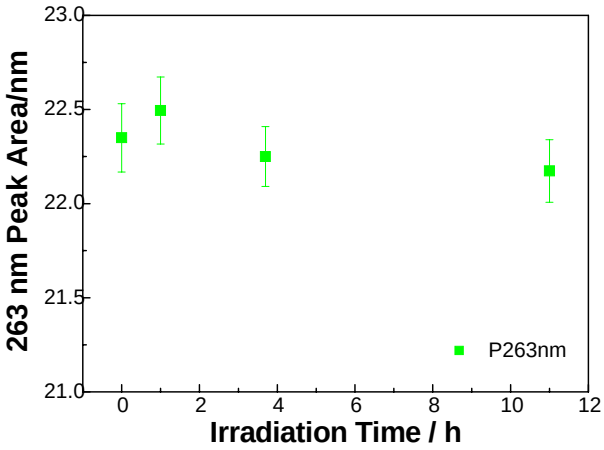

c)

Figure 4 – Paulo J. Gomes et al

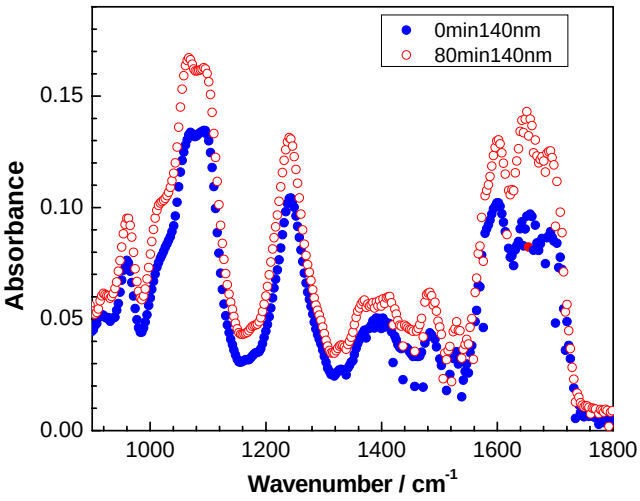

Figure 5 – Paulo J. Gomes et al

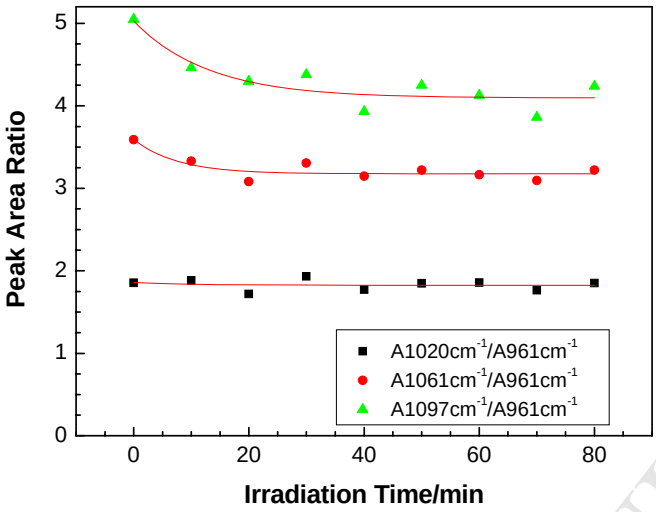

Figure 6 – Paulo J. Gomes et al

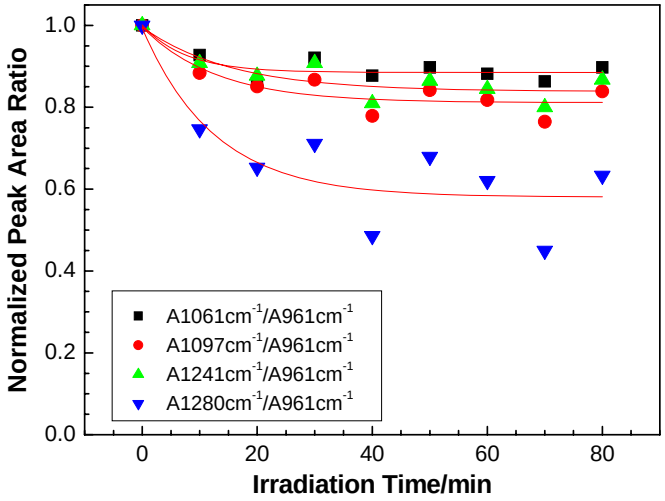

Figure 7 – Paulo J. Gomes et al

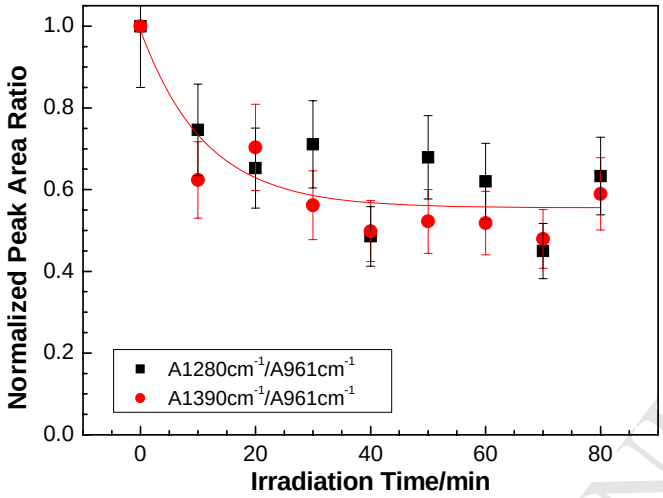

Figure 8 – Paulo J. Gomes et al

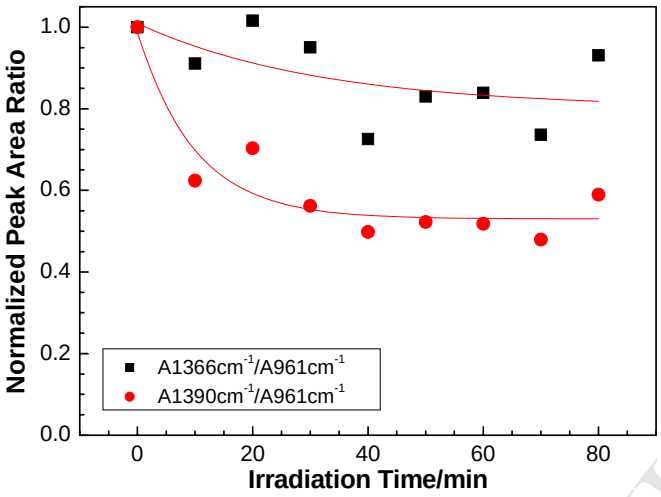

Figure 9 - Paulo J. Gomes et al

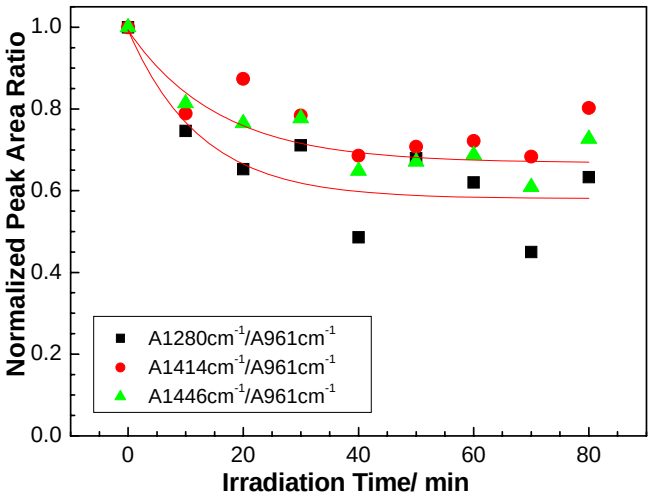

Figure 10 - Paulo J. Gomes et al

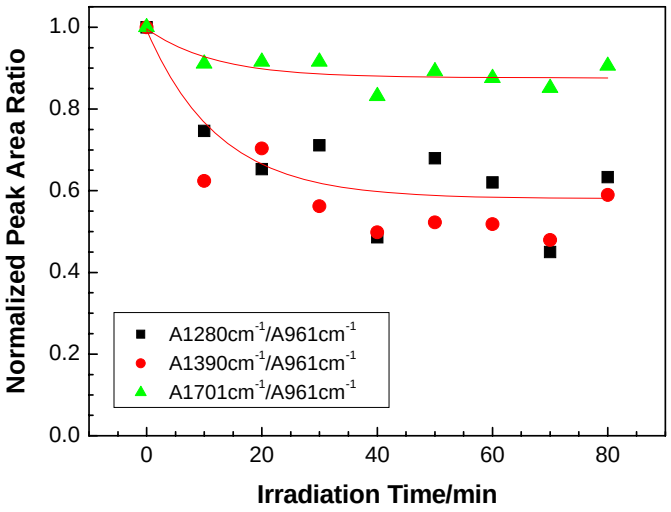

Figure 11 - Paulo J. Gomes et al

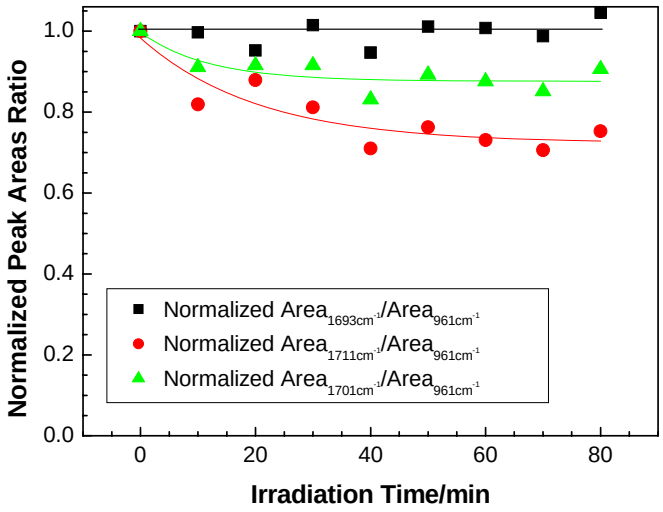

Figure 12 - Paulo J. Gomes et al

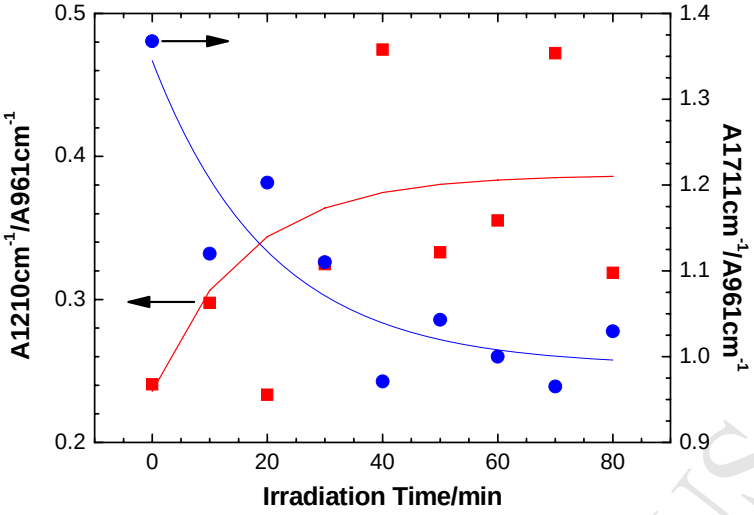

Figure 13 - Paulo J. Gomes et al

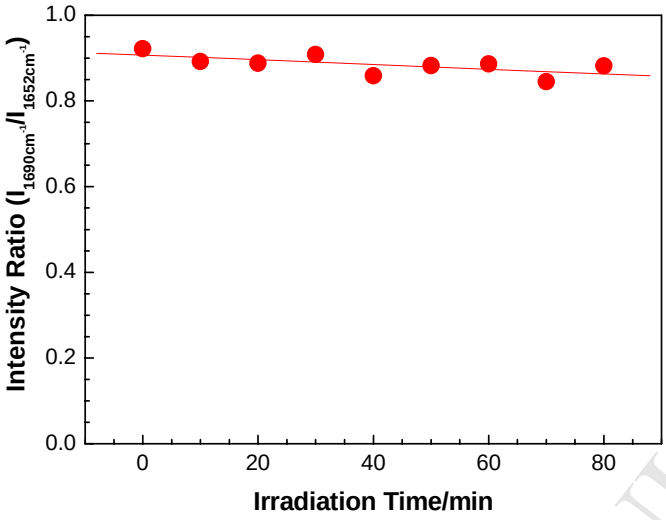

Figure 14 - Paulo J. Gomes et al